STUDYING THE ELECTROCHEMICAL PROPERTIES OF POTASSIUM-DOPED SODIUM-MANGANESE OXIDE CATHODE MATERIALS FOR SODIUM-ION BATTERIES

Van Ky Nguyen[1,3], Van Nghia Nguyen[2,*], Dinh Lam Vu[3], Dinh Thao Vu[1], Trung Son Luong[1]

[1]*Faculty of Physics and Chemical Engineering, Le Quy Don Technical University*

[2]*Research Center of Advanced Materials and Applications, Institute of Architecture, Construction, Urban and Technology, Hanoi Architectural University*

[3]*Graduate University of Science and Technology, Vietnam Academy of Science and Technology*

Abstract

The development of layered sodium manganese oxide cathode materials with high capacity and long life is one of the keys to boosting the performance of sodium-ion batteries (SIBs), but it remains a great challenge. In this work, a potassium doped P2-type sodium manganese oxide, $Na_{0.8}K_{0.1}Mn_{0.9}O_2$ (NKMO), is developed as a high-capacity and long-lasting cathode for high-performance SIBs. Sodium-potassium-manganese oxide $Na_{0.8}K_{0.1}Mn_{0.9}O_2$ was synthesized by a conventional solid-state reaction method. Crystal structure and morphology of the NKMO material were investigated by X-ray diffraction (XRD), scanning electron microscopy (SEM), and energy-dispersive X-ray spectroscopy (EDX). The NKMO material was utilized to fabricate CR2032-type coin cells, and later evaluated for its electrochemical characteristics. The electrochemical characteristics of NKMO were evaluated through cyclic voltammetry (CV), electrochemical impedance spectroscopy (EIS), and galvanostatic charging-discharging (GCD) at different current densities on a NEWARE battery testing system. The NKMO material had a superior initial charge and discharge capacity, approximately 130 $mAh.g^{-1}$ and 125 $mAh.g^{-1}$, respectively, within the voltage range of 1.5-4 V at a current density of 0.1 C. Remarkably, the capacity remained stable at 100 $mAh.g^{-1}$ even after 100 cycles. These findings indicate that NKMO is a highly promising cathode material for sodium-ion batteries.

Keywords: *Sodium-ion battery; sodium manganese oxide; cathode materials; solid-state reaction.*

1. Introduction

The rapidly increasing energy demand has resulted in the aggravating environmental pollution, which has compelled the development of renewable energy resources including geothermal, wind power, and solar energy [1-5]. However, its intrinsic disadvantages of intermittency and regional disparity make it necessary to

[*] Corresponding author email: nghianv@hau.edu.vn
DOI: 10.56651/lqdtu.jst.v2.n02.862.pce

develop reliable large-scale electric energy storage devices [6]. Lithium-ion batteries (LIBs) have been considered as the dominate power supply for consuming electronics and electric vehicles due to thier high energy density and long cycle life. However, the cost of Li is constantly increasing due to its scarcity, so scientists are trying to find alternative sources of materials. Fortunately, sodium-ion batteries (SIBs) could well meet these requirements due to the much higher abundance of sodium in the Earth's crust compared to lithium. Additionally, the similar physical and chemical properties of sodium and lithium make sodium-ion batteries promising candidates in the near future [7, 8].

The structure and operating principles of sodium-ion and lithium-ion batteries are quite similar. However, due to the larger radius of sodium ions compared to lithium ions, the intercalation and extraction capabilities of sodium ions within electrode materials are less efficient. The larger radius of Na^+ ions results in sluggish kinetics, significant volume changes during sodiation and desodiation, lower capacity, and shorter cycle life for sodium-ion batteries (SIBs). Consequently, to develop high-performance SIBs, it is crucial to explore suitable electrode materials, particularly cathode materials with exceptional properties. There are reported cathode materials meeting the requirement such as AMO2, AMPO4 (i.e., A is alkali metals and M is transition metals), and phosphates polyanions [9-23].

Among AMO2-type materials, a variety of P2-type layered-structure materials have been reported for SIBs, primarily due to their superior energy density relative to other materials [9-16]. In particular, manganese-based oxides exhibit moderate electrochemical performance, with a notable emphasis on their high cycling stability. For example, Sauvage *et al.* demonstrated reversible insertion and extraction of Na^+ ions in pure $Na_{0.44}MnO_2$ with an initial capacity of approximately 80 $mAh.g^{-1}$ at 0.1 C. However, after 50 cycles, only half of the original capacity was retained [17]. Some for instance other, Caballero *et al.* reported that P2-$Na_{0.66}MnO_2$ cell had a capacity of 160 $mAh.g^{-1}$, which rapidly decreased to 60 $mAh.g^{-1}$ after 10 cycles [18]; P2-$Na_{0.7}MnO_2$ material showed the similar characteristics in which the capacity of the material was 140 $mAh.g^{-1}$ and remained at 70 $mAh.g^{-1}$ after 20 cycles [19]; P2-type $Na_{0.53}MnO_2$ exhibited a discharge capacity of 120 $mAh.g^{-1}$ at 0.2 C, and the capacity reduced to about 90 mAh g^{-1} after 50 cycles [20].

Doping other transition metals into manganese-based oxide has improved the cycling ability and rate capability of the manganese-based oxide such as Pang *et al*. reported that doping of Co and Cu generated a synergetic improvement of multi-metallic ions that improved electrode kinetics of P2-type $Na_{2/3}Mn_{1/2}Co_{1/3}Cu_{1/6}O_2$ oxide. The material had a capacity of 118.2 $mAh.g^{-1}$ at a current density of 10 $mA.g^{-1}$ and

retained 66% of its capacity after 100 cycles [21]. In addition, Jianyin Wang *et al*. reported that doping Cu of P2 -$Na_{0.7}Mn_{0.9}Cu_{0.1}O_2$ material has achieved a capacity of 130 mAh.g^{-1} at a current 0.1 C, and exhibited a stable cycle performance, also as a capacity retention of 80% obtained after 100 cycles [22].

On the other hand, doping alkaline metals into manganese-based oxide also improved the cycling ability and rate capability of the manganese-based oxide. For example, Liangtao Yang and colleagues had successfully synthesized P2-$Na_{0.67}Mn_{0.6}Ni_{0.2}Li_{0.2}O_2$ in which a partial amount of manganese ions were randomly substituted by the lithium and nickel ions. The P2-$Na_{0.67}Mn_{0.6}Ni_{0.2}Li_{0.2}O_2$ exhibited a specific capacity of 115 mAh.g^{-1} and 80 mAh.g^{-1} at current densities of 0.1 C and 1 C, respectively, and the capacity retained of 95.6% after 100 cycles at 0.1 C [23]. In this work, we doped potassium into sodium manganese oxide-based materials (NKMO). The results showed that the electrochemical properties of NKMO materials were significantly improved. The specific results are presented in the following section.

2. Experiments

2.1. Synthesis of NKMO materials

Potassium-doped sodium-manganese oxide material (NKMO) was synthesized by a solid-state reaction method. A mixture of sodium carbonate (Na_2CO_3, Sigma-Aldrich), potassium carbonate (K_2CO_3, Sigma-Aldrich), and manganese carbonate (MnCO, Sigma-Aldrich) was mixed at a molar ratio of Na:K:Mn = 0.8:0.1:0.9. Then the mixture was ball milled at 100 rpm for 1 hour. The balls used were quartz with a diameter of 8 mm, and the weight ratio of the balls to the materials was 50:1. The obtained mixed powders were heat-treated at 500°C for 10 hours in the air to remove carbonates. The resulting product was then calcined at 750°C for 24 hours to obtain the $Na_{0.8}K_{0.1}Mn_{0.9}O_2$ (NKMO) material. The reaction creating NKMO during calcination can be illustrated by the following equation:

$$8Na_2CO_3 + K_2CO_3 + 18MnCO_3 + 13/2O_2 \rightarrow 20Na_{0.8}K_{0.1}Mn_{0.9}O_2 + 27CO_2$$

Then, the synthesized NKMO materials were analyzed to determine their morphological, structural, and electrochemical properties.

2.2. Material characterizations

The crystal structure of NKMO was verified using X-ray diffraction (XRD) with a Siemens D5005 diffractometer, employing Cu-Kα radiation (λ = 1.54 Å) over a 2θ range of 10-70° with a step size of 0.05°. The morphology of the NKMO material was examined through scanning electron microscopy (SEM) using a JEOL JSM-6490

microscope. The microscope was also used to analyze composition of the NKMO materials via energy dispersive X-ray spectroscopy (EDX).

The electrochemical performance of NKMO was assessed using cyclic voltammetry (CV) and electrochemical impedance spectroscopy (EIS) on a Metrohm Autolab PGSTAT 302 N. The charge-discharge capacities at various current densities, ranging from 1.5 V to 4.0 V, were measured using a NEWARE battery testing system (GCD).

The electrochemical measurements were conducted using CR2032-type sodium-ion batteries, with NKMO as the cathode, sodium foil as the anode, a polypropylene (PE) membrane as the separator, and a solution of 1 M NaClO4 in a mixture of ethylene carbonate/diethylene carbonate (EC/DEC, 1:1 by volume) as the electrolyte. The CR2032 coin cells were assembled in a glove box with oxygen and moisture levels below 0.1 ppm, and stabilized for 24 hours before testing. For the preparation of the electrode materials, a slurry was formed by mixing the active material (NKMO), black carbon (supper P), and polyvinylidene fluoride (PVDF) binder in a weight ratio of 8:1:1 in N-methyl-2-pyrrolidone (NMP). This slurry was then uniformly coated onto 20 μm-thick aluminum foil by tape casting, dried at 100°C in a vacuum oven for 12 hours, and cut into sheets.

3. Results and discussions

3.1. Structural and morphological characterization

The phase structure of the synthesized NKMO materials is illustrated in Fig. 1. As depicted in Fig. 1a, the XRD pattern of the NKMO material can correspond to the hexagonal P2-structure, which belongs to the P63/mmc space group. The diffraction peaks observed at 16.01°, 31.25°, 36.75°, 38.32°, 45.68°, 49.15°, 62.52°, 65.14°, and 67.52° are accurately identified as the (002), (004), (100), (101), (102), (103), (104), (106), (110), and (008) planes, respectively. To extract more valuable information from the XRD data, the lattice parameters were calculated using UnitCell software, and the estimated parameters were a = b = 2.862 Å and c = 11.128 Å. Compared to the JCPDS #27-0751 standard (c = 11.12 Å), the c value of NKMO is higher, indicating a greater distance between the adjacent O-Mn-O slabs in the NKMO [24-27]. This increased distance contributes to the enhanced stability of the NKMO structure. The higher c value results in shift towards lower 2θ angles in the the diffraction peaks. The increase in lattice constant compared to the standard can be attributed to the phase appearance of $Na_{0.612}K_{0.056}MnO_2$ material (a = b = 2.868 Å and c = 11.134 Å), where the larger ionic radii of K^+ compared to Na^+ lead to a larger interlayer space [25]. In addition, we synthesized $Na_{0.8}Mn_{1.0}O_2$ (NMO) material samples under similar conditions to NKMO for comparison. Calculation based on XRD result of the obtained NMO material gave

a = b = 2.862 Å and c = 11.122 Å. The c value of NMO (c = 11.122 Å) is smaller than that of NKMO (c = 11.128 Å).

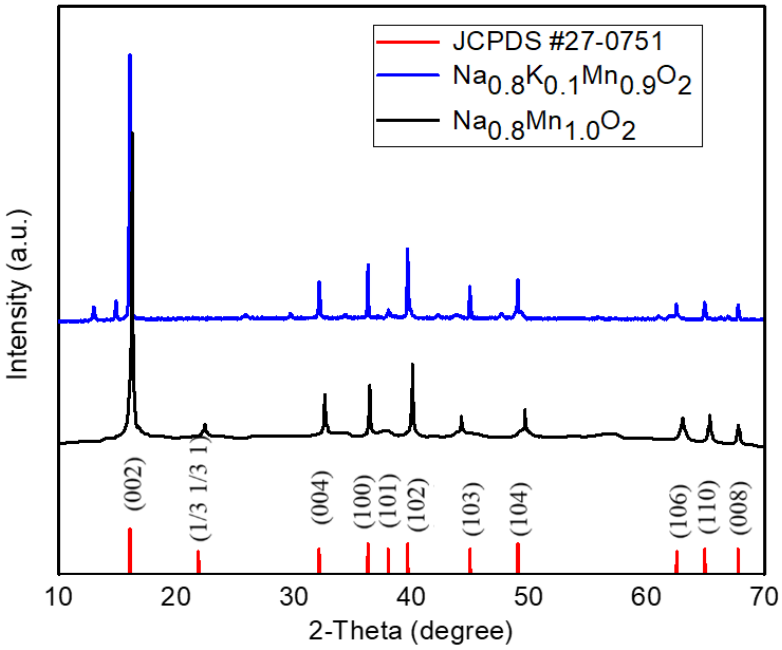

Fig. 1. XRD pattern of NKMO materials.

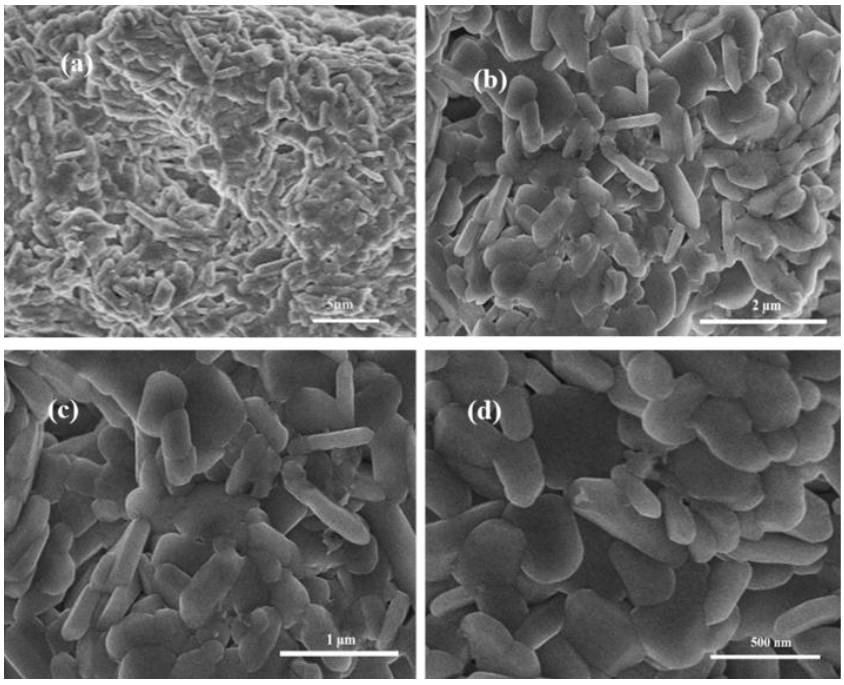

Fig. 2. SEM images of NKMO material at different magnifications; (a) ten thousand times; (b) twenty thousand times; (c) thirty thousand times; (d) fifty thousand times.

The morphology of the NKMO material was confirmed through scanning electron microscopy (SEM), as illustrated in Fig. 2. The SEM images at magnifications of ten thousand times, twenty thousand times, thirty thousand times, and fifty thousand times are displayed in Figures 2a, 2b, 2c, and 2d, respectively. These images reveal that the NKMO material particles are polyhedral in shape, with sizes ranging from 300 nm to 1 µm.

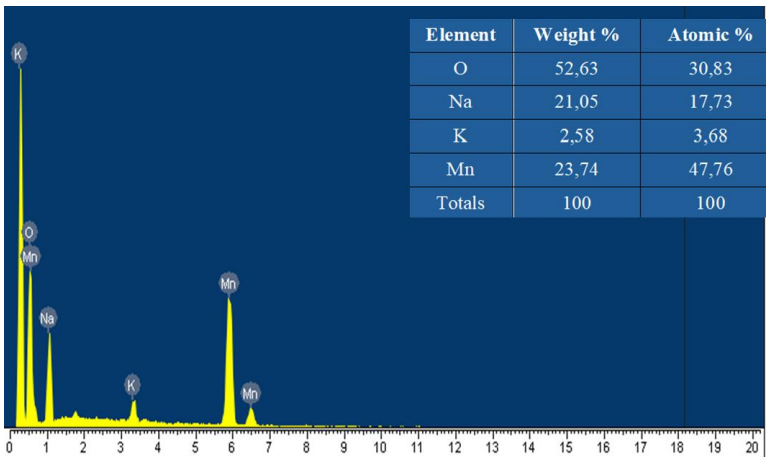

Fig. 3. Energy dispersive X-ray spectroscopy (EDX) result of NKMO.

The composition of the NKMO material was evaluated using energy dispersive X-ray spectroscopy (EDX), as depicted in Fig. 3. The result indicated that the synthesized NKMO material comprised Na, K, Mn, and O elements. The atomic ratio of Na, K, Mn, and O was approximately 0.8:0.1:0.9:2, aligning with the initially used precursor ratio.

3.2. Electrochemical properties

Figure 4a illustrates the charge and discharge profiles of the NKMO material at a current density of 0.1 C (12 $mA.g^{-1}$) within a voltage range of 1.5 to 4.0 V. The overlapping of the initial charge and discharge curves indicates exceptional cyclability of the NKMO material. The charge capacity and discharge capacity of the first cycle are approximately 130 $mAh.g^{-1}$ and 125 $mAh.g^{-1}$, respectively. The charge-discharge curves show two voltage plateaus: 2.0 to 2.75 V and 3.6 to 4.0 V during the charge process, and 3.8 to 3.5 V and 2.6 to 1.6 V during the discharge process. The observed voltage plateaus likely correspond to the oxidation and reduction processes of Mn^{4+}/Mn^{3+} and Mn^{3+}/Mn^{2+} during the charge and discharge processes, respectively [28].

A thorough analysis of the initial three cycles' charging and discharging outcomes reveals that NKMO materials exhibit superior electrochemical properties compared to sodium manganese oxide-based materials. This demonstrates that doping potassium into sodium manganese oxide significantly enhances the sodium ion insertion and extraction

processes. As shown in Table 1, the charge-discharge capacity of NKMO materials surpasses that of various sodium manganese oxide-based materials.

Table 1. Comparison of discharge capacity of NKMO material with previously reported sodium manganese oxide-based materials

Electrode materials	**Discharge capacity (**mAh.g^{-1}**)**	**References**
P2-$Na_{0.44}MnO_2$	101	[18]
P2-$Na_{0.67}Mn_{0.6}Ni_{0.2}Li_{0.2}O_2$	115	[23]
P2-$Na_{0.85}Li_{0.17}Ni_{0.21}Mn_{0.64}O_2$	105	[29]
P2-$Na_{1.0}Li_{0.2}Mn_{0.8}O_2$	112	[30]
P2-$Na_{0.8}Li_{0.12}Ni_{0.22}Mn_{0.66}O_2$	120	[31]
P2-$Na_{0.67}Ni_{0.33}Mn_{0.67}O_2$	86.8	[32]
P2-$Na_{2/3}Mn_{0.67}Ni_{0.22}Cu_{0.05}Ti_{0.02}Al_{0.02}O_2$	107	[33]
P2-$Na_{0.66}Ni_{0.25}Mn_{0.55}Ti_{0.2}O_2$	114	[34]
P2-$Na_{0.67}Mn_{0.65}Ni_{0.2}Mg_{0.15}O_2$	105	[35]
NKMO	125	This study

Figure 4b shows the charge-discharge capacities of the NKMO material over 100 cycles at a current density of 0.1 C. The specific capacity of the material gradually declines to around 100 mAh.g^{-1} by the 100th cycle. The capacity remains about approximately 80% of its initial cycle. The cyclic efficiency of the synthesized NKMO material surpasses that of several reported cathode materials [17-23].

Figures 4c and 4d depict the charge-discharge profiles and specific capacity of NKMO material at various current densities: 0.1 C, 0.2 C, 0.5 C, and 1 C. The discharge capacity notably decreases from approximately 125 mAh.g-1 at 0.1 C (from the 1st to 5th cycle) to around 110 mAh.g^{-1} at 0.2 C (from the 6th to 10th cycle), then to about 80 mAh.g^{-1} at 0.5 C (from the 11th to 15th cycle), and finally to roughly 40 mAh.g^{-1} at 1 C (from the 16th to 20th cycle). Upon reverting the current density back to 0.1 C (from the 21st to 25th cycle), the capacity recovers to about 120 mAh.g^{-1}, demonstrating that the NKMO material maintains structural stability even after undergoing charge-discharge cycles at elevated current densities.

Figure 5a presents the cyclic voltammetry (CV) scan of the NKMO material. The CV scan was conducted over a voltage range of 1.5 to 4.0 V at a scanning rate of 0.2 mV.s^{-1} using the Metrohm Autolab PGSTAT 302 N. During the scan, the working electrode was connected to the battery's positive terminal, while the counter and reference electrodes were connected to the negative terminal.

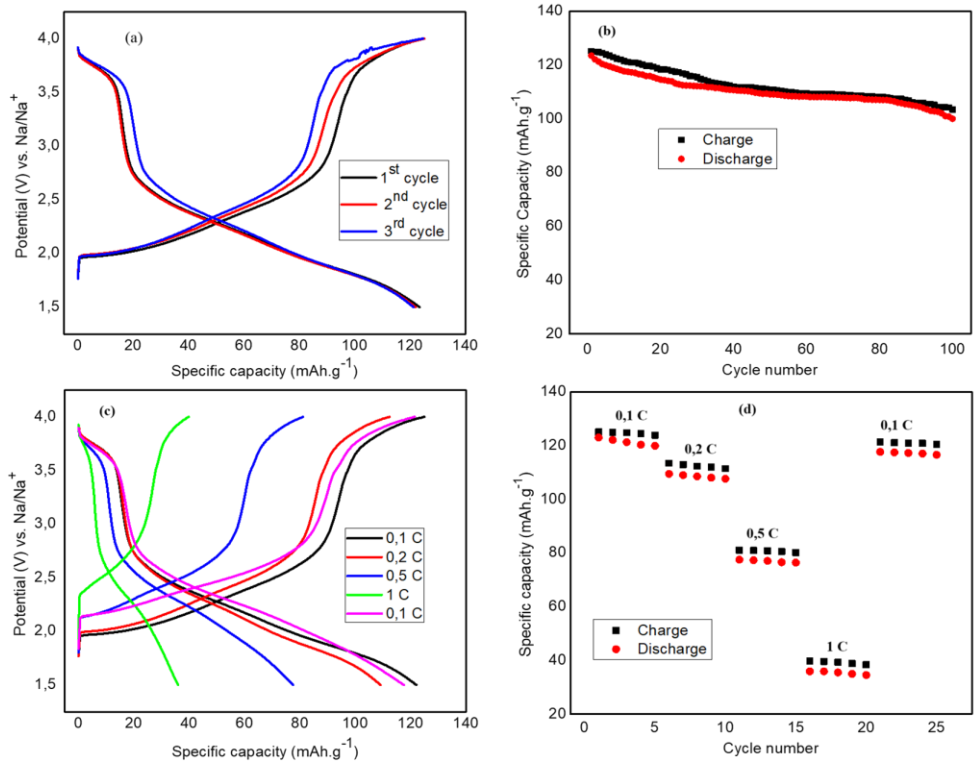

Fig. 4. (a, b) - The charging-discharging profiles of NKMO at 0.1 C;
(c, d) - The charging-discharging profiles at different current densities.

The CV spectrum reveals pairs of peaks corresponding to the voltage plateaus observed during the charge-discharge processes. Peaks at approximately 1.6 V and 2.2 V are indicative of the oxidation and reduction processes of Mn^{3+}/Mn^{2+}, while peaks at 2.75 V and 3.9 V correspond to the oxidation and reduction processes of Mn^{4+}/Mn^{3+} in the NKMO electrode material. The substantial area under these peaks demonstrates the high specific capacities of the NKMO material.

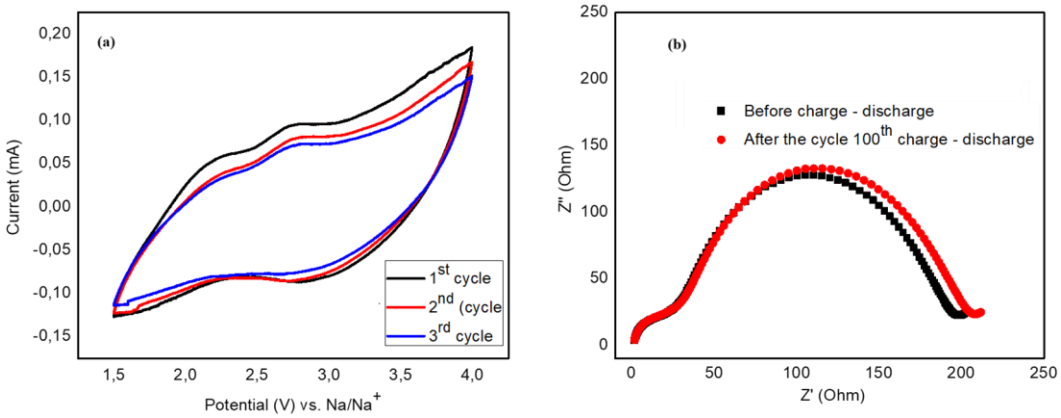

Fig. 5. (a) The CV curves of NKMO at 0.2 mV. s^{-1}; (b) Nyquist plots of the NKMO materials.

The electrochemical impedance spectroscopy (EIS) characterization was performed across a frequency range from 1 MHz to 0.1 Hz to assess the electrochemical reaction kinetics, as depicted in Fig. 5b. The Nyquist plots of the NKMO material, both before the first cycle and after the 100^{th} cycle, exhibit a small semicircle at high frequencies and a larger semicircle at low frequencies. The Nyquist plots of the NKMO material, both before the first cycle and after the 100^{th} cycle, exhibit a small semicircle at high frequencies and a larger semicircle at low frequencies. These semicircles likely correspond to the charge transfer processes involving Mn^{3+}/Mn^{2+} and Mn^{4+}/Mn^{3+}. This behavior is also reflected in the CV spectrum with the corresponding peak pairs and in the charge-discharge curve with the associated voltage plateaus. The total impedance is also relatively low, indicating that the material maintains stability during the reversible intercalation and extraction of Na^+ ions into the NKMO structure.

4. Conclusions

The sodium manganese oxide-based materials are potential cathode materials for sodium-ion batteries. However, these materials experience capacity loss during cycling process due to phase transitions along with the insertion and desertion of Na^+. In this study, we successfully doped potassium into sodium manganese oxide-based materials. The electrochemical properties of sodium manganese oxide-based materials can be significantly improved by doping potassium into them. Our XRD, SEM, and EDS results confirm that the NKMO material has a hexagonal P2-structure, as compared to the JCPDS #27-0751 standard. The NKMO material particles range in size from approximately 300 nm to 1 µm, with a combinatorial formula of $Na_{0.8}K_{0.1}Mn_{0.9}O_2$. The electrochemical properties of NKMO materials are evaluated by cyclic voltammetry (CV), charge-discharge with constant current density, and electrochemical impedance spectroscopy (EIS). The NKMO material has a high specific discharge capacity of 125 $mAh.g^{-1}$ at the first cycle. The discharge capacity remains about 100 $mAh.g^{-1}$ after 100 cycles. The results suggest that the NKMO material is a potential cathode material for sodium-ion batteries.

Acknowledgement

This research is funded by Le Quy Don Technical University Research Fund under the grant number 2023.QHT.01.

References

[1] V. R. Stamenkovic, D. Strmcnik, P. P. Lopes, and N. M. Markovic, "Energy and fuels from electrochemical interfaces", *Nature Materials*, Vol. 16, Iss. 1, pp. 57-69, 2016. DOI: 10.1038/nmat4738

[2] L. Wen, M. Zhou, C. Wang, Y. Mi and Y. Lei, "Nanoengineering energy conversion and storage devices via atomic layer deposition", *Advanced Energy Materials*, Vol. 6, 2016. DOI: 10.1002/aenm.201600468

[3] N. Ortiz-Vitoriano, N. E. Drewett, E. Gonzalo, and T. Rojo, "High performance manganese-based layered oxide cathodes: Overcoming the challenges of sodium ion batteries", *Energy & Environmental Science*, Vol. 10, 2017, pp. 1051-1074. DOI: 10.1039/C7EE00566K

[4] X. Wang, H. M. Kim, Y. Xiao, and Y. K. Sun, "Nanostructured metal phosphide-based materials for electrochemical energy storage", *Journal of Materials Chemistry A*, Vol. 4, pp. 14915-14931, 2016. DOI: 10.1039/C6TA06705K

[5] Y. Zhao, X. Li, B. Yan *et al.*, "Hierarchical multi-metal-doped mesoporous NiO-silica nanoparticles towards a viable platform for Li-ion battery electrode application", *Advanced Energy Materials*, Vol. 6, 2016, 1502175, https://link.springer.com/article/10.1007/s11814-021-1003-1

[6] Y. Liu, D. He, R. Han, G. Wei, and Y. Qiao, "Nanostructured potassium and sodium ion incorporated Prussian blue frameworks as cathode materials for sodium-ion batteries", *Chemical Communications*, Vol. 53, pp. 5569-5572, 2017. DOI: 10.1039/C7CC02303K

[7] Y. You and A. Manthiram, "Progress in high-voltage cathode materials for rechargeable sodium-ion batteries", *Advanced Energy Materials*, Vol. 8, 2018, 1701785. DOI: 10.1002/aenm.201701785

[8] B. Peng, Z. Sun, S. Jiao *et al.*, "Facile self-templated synthesis of P2-type $Na_{0.7}CoO_2$ microsheets as long-term cathode for high-energy sodiumion battery", *Journal of Materials Chemistry A*, Vol. 175, pp. 2050-7488, 2019. DOI: 10.1039/C9TA02966D

[9] D. Carlier, J. H. Cheng, R. Berthelot *et al.*, "The P2-$Na_{2/3}Co_{2/3}Mn_{1/3}O_2$ phase: Structure, physical properties and electrochemical behavior as positive electrode in sodium battery", *Dalton Transactions*, Vol. 40, Iss. 36, pp. 9306-9312, 2011. DOI: 10.1039/C1DT10798D

[10] R. J. Clément, J. Billaud, A. R. Armstrong *et al.*, "Structurally stable Mg-doped P2-$Na_{2/3}Mn_{1-y}Mg_yO_2$ sodium-ion battery cathodes with high rate performance: insights from electrochemical, NMR and diffraction studies", *Energy and Environmental Science*, Vol. 9, Iss. 10, 2016, pp. 3240-3251. DOI: 10.1039/C6EE01750A

[11] K. Tang, Y. Wang, X. Zhang *et al.*, "High-performance P2-type Fe/Mn-based oxide cathode materials for sodium-ion batteries", *Electrochimica Acta*, Vol. 312, 2019. DOI: 10.1016/j.electacta.2019.04.183

[12] J. Li, J. Wang, X. He *et al.*, "P2-type $Na_{0.67}Mn_{0.8}Cu_{0.1}Mg_{0.1}O_2$ as a new cathode material for sodiumion batteries: Insights of the synergetic effects of multi-metal substitution and electrolyte optimization", *Journal of Power Sources*, Vol. 416, 2019, pp. 184-192. DOI: 10.1016/j.jpowsour.2019.01.086

[13] L. Bi, Z. Miao, X. Li *et al.*, "Improving electrochemical performance of $Na_3(VPO_4)_2O_2F$ cathode materials for sodium ion batteries by constructing conductive scaffold", *Electrochimica Acta*, Vol. 337, 20 March 2020. DOI: 10.1016/j.electacta.2020.135816

[14] T. T. H. Nguyen, V. N. Nguyen, V. K. Nguyen *et al.*, "Synthesis and electrochemical characteristics of zinc-doped sodium manganese oxide as a cathode material for sodium-ion batteries", *Journal of Science and Technique - Section on Physics and Chemical Engineering*, Vol. 1, No. 01, 2023, pp. 1859-0209. DOI: 10.56651/lqdtu.jst.v1.n01.623.pce

[15] N. Bucher, S. Hartung, I. Gocheva *et al.*, "Combustion-synthesized sodium manganese (cobalt) oxides as cathodes for sodium ion batteries", *Journal of Solid State Electrochemistry*, Vol. 17, Iss. 7, pp. 1923-1929, 2013. DOI: 10.1007/s10008-013-2047-x

[16] N. Yabuuchi, M. Kajiyama, J. Iwatate *et al.*, "P2-type $Na_x[Fe_{1/2}Mn_{1/2}]O_2$ made from earth-abundant elements for rechargeable Na batteries", *Nature Materials*, Vol. 11, pp. 512-517, 2012. https://www.nature.com/articles/nmat3309

[17] X. He, J. Wang, B. Qiu *et al.*, "Durable high-rate capability $Na_{0.44}MnO_2$ cathode material for sodium-ion batteries", *Nano Energy*, Vol. 27, pp. 602-610, 2016. DOI: 10.1016/j.nanoen.2016.07.021

[18] K. Y. Shen, M. Lengyel, L. Wang, and R. L. Axelbaum, "Spray pyrolysis and electrochemical performance of $Na_{0.44}MnO_2$ for sodium-ion battery cathodes", *MRS Communications*, Vol. 7, Iss. 1, pp. 74-77, 2017. DOI: 10.1557/mrc.2017.4

[19] A. Caballero, L. Hernán, J. Morales *et al.*, "Synthesis and characterization of high-temperature hexagonal P2-$Na_{0.6}MnO_2$ and its electrochemical behaviour as cathode in sodium cells", *Journal of Materials Chemistry*, Vol. 12, Iss. 4, pp. 1142-1147, 2002. DOI: 10.1039/b108830k

[20] J. Y. Li, H. Y. Lü, X. H. Zhang *et al.*, "P2-type $Na_{0.53}MnO_2$ nanorods with superior rate capabilities as advanced cathode material for sodium ion batteries", *Chemical Engineering Journal*, Vol. 316, pp. 499-505, 2017. DOI: 10.1016/j.cej.2017.01.109

[21] J. Li, J. Wang, X. He *et al.*, "P2-type $Na_{0.67}Mn_{0.8}Cu_{0.1}Mg_{0.1}O_2$ as a new cathode material for sodiumion batteries: Insights of the synergetic effects of multi-metal substitution and electrolyte optimization", *Journal of Power Sources*, Vol. 416, pp. 184-192, 2019. DOI: 10.1016/j.jpowsour.2019.01.086

[22] J. Wang, H. Liu, Q. Yang *et al.*, "Cu-doped P2-$Na_{0.7}Mn_{0.9}Cu_{0.1}O_2$ sodium-ion battery cathode with enhanced electrochemical performance: Insight from water sensitivity and surface Mn(II) formation studies", *ACS Applied Materials & Interfaces*, Vol. 10, pp. 1-25, 2020. DOI: 10.1021/acsami.0c07244

[23] L. Yang, L. Y. Kuo, J. M. L. del Amo *et al.*, "Structural aspects of P2-type $Na_{0.67}Mn_{0.6}Ni_{0.2}Li_{0.2}O_2$ (MNL) stabilization by lithium defects as a cathode material for sodium-ion batteries", *Advanced Functional Materials*, Vol. 31, Iss. 38, 2021, 2102939. DOI: 10.1002/adfm.202102939

[24] N. V. To, K. V. Nguyen, H. S. Nguyen *et al.*, "P2-type layered structure $Na_{1.0}Li_{0.2}Mn_{0.7}Ti_{0.1}O_2$ as a superb electrochemical performance cathode material for sodium-ion batteries", *Journal of Electroanalytical Chemistry*, Vol. 880, 2021, 114834. DOI: 10.1016/j.jelechem.2020.114834

[25] C. Wang, L. Liu, S. Zhao *et al.*, "Tuning local chemistry of P2 layered-oxide cathode for high energy and long cycles of sodium-ion battery", *Nature Communications*, Vol. 12, Iss. 1, pp. 1-10, 2021. DOI: 10.1038/s41467-021-22523-3

[26] J. P. Parant, R. Olazcuaga, M. Devalette, C. Fouassier, and P. Hagenmuller, "Sur quelques nouvelles phases de formule Na_xMnO_2 ($x \leqslant 1$)", *Journal of Solid State Chemistry*, Vol. 3, Iss. 1, 1971, pp. 1-11. DOI: 10.1016/0022-4596(71)90001-6

[27] W. Zhao, A. Tanaka, K. Momosaki *et al.*, "Enhanced electrochemical performance of Ti substituted P2-$Na_{2/3}Ni_{1/4}Mn_{3/4}O_2$ cathode material for sodium ion batteries", *Electrochimica Acta*, Vol. 170, pp. 171-181, 2015. DOI: 10.1016/j.electacta.2015.04.125

[28] D. Sehrawat, A. Rawal, S. Cheong *et al.*, "Alkali metal-modified P2 Na_xMnO_2: crystal structure and application in sodium-ion batteries", *Inorganic Chemistry*, Vol. 59, Iss. 17, pp. 11847-12960, 2020. DOI: 10.1021/acs.inorgchem.0c01078

[29] D. Kim, S. H. Kang, M. Slater *et al.*, "Enabling sodium batteries using lithium substituted sodium layered transition metal oxide cathodes", *Advanced Energy Materials*, Vol. 1, Iss. 3, pp. 333-336, 2011. DOI: 10.1002/aenm.201000061

[30] T. T. H. Nguyen, V. K. Nguyen, T. S. Luong *et al.*, "Facile synthesis of cobalt-doped sodium lithium manganese oxide with superior rate capability and excellent cycling performance for sodium-ion battery", *Journal of Electroanalytical Chemistry*, Vol. 929, 2023, 117129. DOI: 10.1016/j.jelechem.2022.117129

[31] J. Xu, D. H Lee, R. J. Clément *et al.*, "Identifying the critical role of Li substitution in P2–Na_x $[Li_yNi_zMn_{1-y-z}]O_2$ ($0 < x, y, z < 1$) intercalation cathode materials for high-energy Na-ion batteries", *Chemistry of Materials*, Vol. 26, Iss. 2, pp. 1260-1269, 2014. DOI: 10.1021/cm403855t

[32] Y. Xie, E. Gabriel, L. Fan *et al.*, "Role of lithium doping in P2- $Na_{0.67}Ni_{0.33}Mn_{0.67}O_2$ for sodium-ion batteries", *Chemistry of Materials*, Vol. 33, Iss. 12, pp. 4445-4455, 2021. DOI: 10.1021/acs.chemmater.1c00569

[33] F. Fu, P. Liu, and H. Wang, "Multicomponent P2-type $Na_{2/3}Mn_{0.67}Ni_{0.22}Cu_{0.05}Ti_{0.02}Al_{0.02}O_2$ as an ultralong cycle-life and superior rate cathode for sodium-ionbatteries", *Materials Letters*, Vol. 253, pp. 124-127, 2019. DOI: 10.1016/j.matlet.2019.06.013

[34] W. Zhao, A. Tanaka, K. Momosaki *et al.*, "Enhanced electrochemical performance of Ti substituted P2-$Na_{2/3}Ni_{1/4}Mn_{3/4}O_2$ cathode material for sodium ion batteries", *Electrochimica Acta*, Vol. 170, pp. 171-181, 2015. DOI: 10.1016/j.electacta.2015.04.125

[35] Y. Wen, J. Fan, C. Shi *et al.*, "Probing into the working mechanism of Mg versus Co in enhancing the electrochemical performance of P2-type layered composite for sodium-ion batteries", *Nano Energy*, Vol. 60, pp. 162-170, 2019. DOI: 10.1016/j.nanoen.2019.02.074

NGHIÊN CỨU TÍNH CHẤT ĐIỆN HÓA CỦA VẬT LIỆU CATỐT OXIT NATRI-MANGAN PHA TẠP KALI CHO PIN NATRI-ION

Nguyễn Văn Kỳ[1,3], Nguyễn Văn Nghĩa[2], Vũ Đình Lãm[3],
Vũ Đình Thảo[1], Lương Trung Sơn[1]

[1]*Khoa Hóa - Lý kỹ thuật, Trường Đại học Kỹ thuật Lê Quý Đôn*

[2]*Trung tâm Nghiên cứu Vật liệu tiên tiến và Ứng dụng, Viện Công nghệ Kiến trúc, Xây dựng và Đô thị, Trường Đại học Kiến trúc Hà Nội*

[3]*Học viện Khoa học và Công nghệ, Viện Hàn lâm Khoa học và Công nghệ Việt Nam*

Tóm tắt: Việc phát triển vật liệu cực dương oxit natri mangan nhiều lớp có dung lượng cao và tuổi thọ dài là một trong những chìa khóa để tăng hiệu suất của pin ion natri (SIB), nhưng vẫn là một thách thức lớn. Trong bài báo này, một oxit natri mangan loại P2 pha tạp kali, $Na_{0,8}K_{0,1}Mn_{0,9}O_2$ (NKMO), được phát triển như một vật liệu cực dương có dung lượng cao và tuổi thọ dài cho SIB hiệu suất cao. Oxit natri-kali-mangan $Na_{0,8}K_{0,1}Mn_{0,9}O_2$ được tổng hợp bằng phương pháp phản ứng trạng thái rắn thông thường. Cấu trúc tinh thể và hình thái của vật liệu NKMO đã được nghiên cứu bằng phương pháp nhiễu xạ tia X (XRD), kính hiển vi điện tử quét (SEM) và quang phổ tán xạ năng lượng tia X (EDX). Vật liệu NKMO được sử dụng để chế tạo pin dạng đồng xu loại CR2032 và sau đó được đánh giá các đặc tính điện hóa thông qua các phép đo quét thế vòng tuần hoàn (CV), phép đo phổ trở kháng điện hóa (EIS) và phép sạc-xả ở các mật độ dòng điện khác nhau. Vật liệu NKMO có dung lượng sạc và xả ban đầu vượt trội lần lượt là 125 $mAh.g^{-1}$ và 123 $mAh.g^{-1}$ trong khoảng 1,5 - 4 V ở mật độ dòng điện 0,1 C. Dung lượng vẫn được duy trì ở mức 100 $mAh.g^{-1}$ sau 100 chu kỳ. Kết quả cho thấy vật liệu NKMO là vật liệu cực dương đầy hứa hẹn cho pin ion natri.

Từ khóa: *Pin natri-ion; natri mangan oxit; vật liệu catốt; phản ứng trạng thái rắn.*

Received: 03/09/2024; Revised: 08/10/2024; Accepted for publication: 30/10/2024

❑